PHYSICAL REVIEW C **66**, 044305 (2002)

Evidence for triaxial deformation near $N=86$: Collective bands in ^{152,153}Dy and ^{153}Ho

D. E. Appelbe,[1,2,3] P. J. Twin,[3] C. W. Beausang,[3,*] D. M. Cullen,[3,†] D. Curien,[4] G. Duchêne,[4]
S. Ertürk,[3,‡] Ch. Finck,[4,§] B. Haas,[4] E. S. Paul,[3] D. C. Radford,[5] C. Rigollet,[4] M. B. Smith,[3,‖] O. Stezowski,[4,¶]
J. C. Waddington,[2] and A. N. Wilson,[6,**]
[1]*CLRC Daresbury Laboratory, Daresbury, Warrington WA4 4AD, United Kingdom*
[2]*Department Physics and Astronomy, McMaster University, Hamilton, Ontario, Canada L8S 4M1*
[3]*Oliver Lodge Laboratory, University of Liverpool, Liverpool L69 7ZE, United Kingdom*
[4]*Institut de Recherches Subatomiques, F-67037 Strasbourg Cedex, France*
[5]*Physics Division, Oak Ridge National Laboratory, Oak Ridge, Tennessee 37831*
[6]*C.S.N.S.M., IN2P3-C.N.R.S., F-91405 Orsay Campus, France*
(Received 22 November 2000; revised manuscript received 17 April 2002; published 18 October 2002)

The $N=86,87$ isotopes of dysprosium and holmium have been investigated using the Eurogam II γ-ray spectrometer. A new collective rotational band has been observed in ^{153}Ho and the previously observed $\nu i_{13/2}$ band in ^{153}Dy has been extended to much higher spin. Comparing these bands and similar bands in ^{152}Dy with the collective bands in the $N=90$ isotopes of Dy, Ho, and Er suggests that the first $h_{11/2}$ proton crossing is not observed at $N=86,87$. This observation has led to the reinterpretation of four of the previously observed bands in ^{152}Dy. It is proposed that the low deformation collective bands in ^{152,153}Dy and ^{153}Ho are associated with a triaxial shape with large positive gamma and that they have a similar origin to the recently observed triaxial superdeformed bands in $^{163-165}$Lu.

DOI: 10.1103/PhysRevC.66.044305 PACS number(s): 21.10.Re, 23.20.En, 23.20.Lv, 27.70.+q

I. INTRODUCTION

Studies of the isotopes of Dy ($Z=66$) and Ho ($Z=67$) have revealed that rare-earth nuclei can exhibit a wide variety of nuclear shapes and structures [1–7]. In the dysprosium nuclei, near the $N=82$ spherical shell closure, the dominant shape at low excitation energies is of an oblate single-particle nature with quasivibrational characteristics. At larger neutron numbers ($N>89$) the yrast states arise from moderately deformed collective rotors ($\beta_2\approx0.2$) [8]. At very high spin some of the more neutron-deficient nuclei (^{151}Dy,^{152}Dy,^{153}Dy) [9,10] become superdeformed (SD). In ^{152}Dy there are three collective bands which coexist with the oblate single-particle states at low spin. These bands have been associated with moderately deformed rotational structures [11,12]. As ^{153}Dy and ^{153}Ho have an additional proton and neutron relative to ^{152}Dy, respectively, one would expect them to also exhibit the three structures observed in ^{152}Dy. Single-particle and SD structures have been reported in both nuclei [4,9,13,14], and in ^{153}Dy a collective band based on an $i_{13/2}$ neutron has been observed [13,15]. In contrast, in ^{153}Ho, no experimental evidence has previously been presented for a moderately deformed collective band, although previous studies [14] have noted the similarity of its single-particle level scheme to that of ^{152}Dy.

This paper reports the first observation of a moderately deformed collective rotational band in the nucleus $^{153}_{67}$Ho$_{86}$, and on the extension of the ^{153}Dy band up to $J^\pi=\frac{101}{2}{}^+\hbar$. Both of these bands are discussed in terms of the cranked shell model and compared with similar bands in the adjacent dysprosium and holmium nuclei. It is proposed that the moderately deformed bands in ^{152,153}Dy and ^{153}Ho are associated with a triaxial shape ($\beta_2\approx0.3$ and $\gamma\approx20°$). The relationship of these triaxial bands with the highly deformed (or superdeformed) triaxial bands ($\beta_2\approx0.4$ and $\gamma\approx20°$) in ^{163,164,165}Lu and ^{154}Er is discussed. One of the bands in ^{152}Dy which previously was assigned as superdeformed has been identified as a candidate for a highly deformed triaxial band.

II. EXPERIMENTAL DETAILS

The data presented here were obtained from two separate experiments, performed with the EUROGAM II γ-ray spectrometer [16] at the IReS Strasbourg. This array comprised 30 Compton suppressed HPGe coaxial detectors [17] which were situated at angles of 22.4°, 46.4°, 133.6°, and 157.6° with respect to the beam direction, and 24 Clover detectors [18] placed in two symmetric rings about 90°.

High-spin states in ^{153}Ho were populated via the ^{120}Sn(^{37}Cl,4n)^{153}Ho fusion-evaporation reaction, at a bombarding energy of 177 MeV. The ^{37}Cl beam was provided by the Vivitron electrostatic tandem accelerator and was incident upon two stacked, self-supporting targets of ^{120}Sn, each

*Present address: W.N.S.L., Physics Department, Yale University, 272 Whitney Avenue, New Haven, CT 06511.

†Present address: Department of Physics and Astronomy, University of Manchester, Manchester M13 9PL, United Kingdom.

‡Present address: Nigde Universitesi, Fen-Edebiyat Fakültesi, Fizik Bölümü, Nigde, Turkey.

§Present address: G.S.I, Plankstrasse 1, 64291 Darmstadt, Germany.

‖Present address: Department of Physics and Astronomy, Rutgers University, New Brunswick, NJ 08903.

¶Present address: Institute de Physique Nucleaire, 43 Boulevard du 11 Novembre 1918, 69622 Villeurbanne Cedex, France.

**Present address: Department of Physics, University of York, Heslington, York YO10 5DD, United Kingdom.

of nominal thickness 440 μg cm^{-2}. Approximately 7.7 $\times 10^8$ events of escape suppressed fold $\geqslant 4$ were collected during the experiment. The $4n$ exit channel, ^{153}Ho, was the most intensely populated, carrying $\approx$45% of the total evaporation cross-section. For comparison, the ^{154}Ho($3n$), ^{152}Ho ($5n$), ^{153}Dy ($p3n$), ^{152}Dy ($p4n$), and ^{150}Tb ($\alpha 3n$) channels carried $\approx$2%, 3%, 8%, 10%, and 22% of the total reaction intensity, respectively.

High-spin states in ^{153}Dy were populated via the ^{124}Sn (^{34}S,5n)^{153}Dy fusion-evaporation reaction at a bombarding energy of 182 MeV. A total of 3.2×10^9 events of escape suppressed fold $\geqslant 5$ were collected during this run. The details of this reaction has been described previously, and can be found in Sec. II of Ref. [12].

III. RESULTS

A. ^{153}Ho

These data were sorted into an E_γ-E_γ-E_γ three dimensional coincidence "cube" for analysis with the LEVIT8R [19] software. A search for rotational bands was performed with the automatic search algorithms described in Refs. [20–22]. As a result of these searches four rotational bands were observed and assigned to the nucleus ^{153}Ho. Three of these bands were consistent with superdeformed bands and have been discussed in Ref. [4]. The remaining band has similar properties to the low-lying rotational bands in ^{152}Dy [12]. The assignment of this band to the nucleus ^{153}Ho has been confirmed on the basis of coincidence relationships between band members and transitions in the known level scheme (the 913-, 632-, 363-, 456-, and 762-keV transitions) [14].

A γ-ray coincidence spectrum of this band, obtained by summing all possible combinations of double gates for transitions in the band, is presented in Fig. 1. The band consists of nine γ-ray transitions spanning the energy range $806 \leqslant E_\gamma \leqslant 1343$ keV (Table I), with an average energy separation of $\Delta E_\gamma \approx 65$ keV. This band is populated with a similar intensity ($\approx$0.7%) to the yrast SD band in ^{153}Ho [4]. The in-band γ-ray separation is larger than that for SD bands in this region ($\Delta E_\gamma \approx 50$ keV), but it is similar to that observed for the moderately deformed bands in ^{152}Dy [11,12] ($\Delta E_\gamma \approx 65$ keV), suggesting that this band is *not* a SD band.

The multipolarities of the in-band transitions have been established from the asymmetry ratio [23], defined as

$$R_{asym} = \frac{I_\gamma(\text{Phase I})}{I_\gamma(\text{Clover})}.$$

Using this method, known stretched quadrupole transitions ($\Delta I = 2$) have $R_{asym} = 1.0$, while stretched dipole transitions ($\Delta I = 1$) were observed to have $R_{asym} = 0.5$. The values of R_{asym} extracted for the in-band members are shown in Table I, and are consistent with the R_{asym} expected for a sequence of stretched quadrupole transitions. Due to the relatively weak intensity of this band a definite decay path to the yrast states in ^{153}Ho could not be determined. Although this band has many γ rays with similar energies to ^{152}Dy(B) [12], the

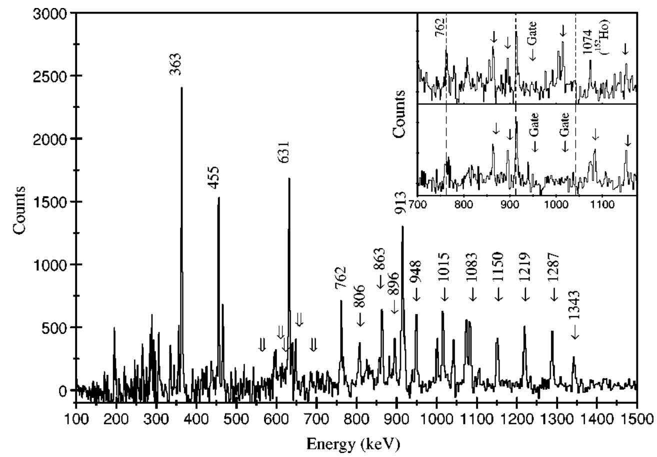

FIG. 1. A spectrum of the rotational band in ^{153}Ho obtained by setting double gates on all pairs of transitions in the band (948 $\rightarrow$1343). The band members are marked by an arrow and their transition energy. Transitions in the decay of the ^{153}Ho spherical states are marked by their transition energies. The double arrows mark the expected position of transitions in ^{152}Dy. The upper inset shows the result of setting a double gate on the 948- and 1083-keV transitions. Band members are marked by an arrow. The lower inset is as for the upper, but the result of a double gate set on the 948- and 1015-keV band members.

fact that γ rays associated with the decay of ^{152}Dy do not appear in Fig. 1 indicates that the assignment of this band to ^{153}Ho is correct. Most of the intensity of the band passes through the 762-keV transition, while a minimal fraction was found to be in coincidence with the 1043-keV transition. This implies one of two possibilities; either the ordering of the 762- and 1043-keV transitions are reversed when compared with the level scheme of Radford *et al.* [14], or one of the decay out transitions is a 762-keV γ ray. The latter implies that the lower lying states assigned to this band would be yrast, which is considered unlikely as these states are previously unreported. Thus the former hypothesis appears likely; such a reassignment is not precluded by the analysis of Radford [14].

B. ^{153}Dy

These data were also sorted into an E_γ-E_γ-E_γ coincidence cube for analysis. A sample double gated spectrum of the extended $i_{13/2}$ band observed in ^{153}Dy is presented in Fig. 2. The spectrum was obtained from summing all possible combinations of double gates resulting from the combination of two lists of energies, excluding the diagonal gates (718.6, 759.3, 799.2, 840.2, 886.9, and 937.8) and the (840.2, 886.9, 937.8, 993.8, 1051.4, 1110.5, 1170.8, and 1230.3) in the coincidence cube. This produces a very clean spectrum of the band. Two transitions that are not associated with the band are clearly visible ($E_\gamma = 636$ keV and $E_\gamma = 213$ keV) in Fig. 2. These transitions have been previously assigned to ^{153}Dy [24], and definitively places this band in ^{153}Dy. The 75.6-keV transition associated with the decay of this band to the 636 keV $\frac{11}{2}^-$ level could not be observed in these data due to absorbers placed in front of the HPGe detectors. The mea-

TABLE I. The measured transition energies, relative intensities, and R_{asym} ratios for the observed bands in ^{153}Ho and ^{153}Dy. The intensity measurements for ^{153}Ho have been normalized to the 1218.7-keV transition, those for ^{153}Dy have been normalized to the 447.3-keV transition. The 1515-keV transition is tentative.

^{153}Ho			^{153}Dy	
Energy (keV)	Intensity	R_{asym}	Energy (keV)	Intensity
			447.3 (4)	100 (5)
			487.6 (4)	84 (5)
			532.0 (4)	127 (5)
			581.1 (4)	97 (5)
			626.8 (4)	93 (5)
			674.2 (4)	81 (5)
			718.6 (4)	79 (5)
			759.3 (5)	41 (6)
			799.2 (5)	42 (6)
			840.2 (5)	37 (6)
806.2 (13)	32 (1)		886.9 (5)	31 (6)
862.9 (6)	62 (2)	0.85 (4)	937.8 (5)	26 (6)
947.8 (13)	91 (3)	0.94 (4)	993.8 (5)	25 (5)
1014.6 (6)	90 (3)	0.88 (3)	1051.4 (6)	17 (5)
1082.6 (5)	88 (2)	1.25 (25)	1110.5 (6)	17 (4)
1150.2 (5)	70 (2)	0.97 (3)	1170.8 (6)	15 (4)
1218.7 (5)	100 (2)	0.73 (3)	1230.3 (6)	11 (4)
1287.4 (5)	67 (2)	0.97 (4)	1288.1 (7)	9 (3)
1342.9 (7)	59 (2)	1.21 (5)	1344.3 (7)	7 (3)
			1399.5 (7)	7 (3)
			1457.9 (10)	
			1515 (2)	
Spin assignment			Spin assignment	
806 keV $\frac{57}{2}^- \rightarrow \frac{53}{2}^-$			447 keV $\frac{17}{2}^+ \rightarrow \frac{13}{2}^+$	
1342 keV $\frac{89}{2}^- \rightarrow \frac{65}{2}^-$			1515 keV $\frac{101}{2}^+ \rightarrow \frac{97}{2}^+$	

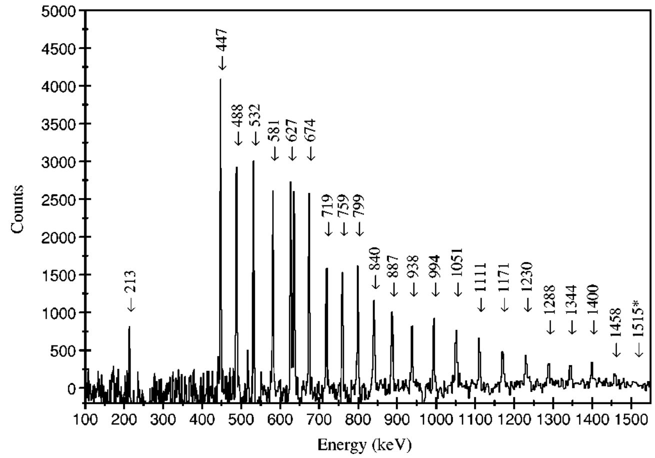

FIG. 2. A spectrum of the $i_{13/2}$ band in ^{153}Dy obtained by setting all possible combinations of double gates between the (717, 759, 799, 840, 887, and 938) and the (840, 887, 938, 994, 1051, 1111, 1171, and 1230) transitions. All the transitions in the band are labeled by their respective energies. The unmarked peak in the spectrum at 636 keV is from ^{153}Dy, and represents the decays from spherical levels fed by this band.

sured transition energies, and relative intensities for the in-band transitions are presented in Table I.

IV. DISCUSSION

While nuclei such as ^{153}Ho can be characterized as predominantly single-particle in nature at low spin, the observation of rotational bands in this region of the Segré chart is not new. Nuclei in the vicinity of the $Z=64$ subshell closure such as ^{151}Gd [25], ^{152}Dy [11,12], and ^{153}Dy [15,26] are known to possess collective rotational bands at low excitation energies based on the occupation of $\nu i_{13/2}$ intruder orbitals. Nuclei with $N\geqslant 90$ are well established as good rotors [2], and in all of these cases orbitals arising from the $\nu i_{13/2}$ shell play an important role in determining the observed characteristics. Those Dy and Ho nuclei with $N\leqslant 90$ exhibit characteristics of both collective and single-particle modes. In these nuclei comparisons between theoretical predictions and the experimentally observed behavior has been remarkably consistent. For example, total Routhian surface (TRS) calculations [27] for ^{156}Dy indicate that a single minimum in the potential energy surface (PES), Fig. 3(a), persists up to the highest rotational frequencies. The deformation parameters predicted for this minimum, $\beta_2=0.23$, $\gamma=0°$, are in remarkable agreement with those determined experimentally [28]. At this deformation it is expected that several gains in aligned angular momentum, or ''alignments,'' resulting from paired band crossings will occur. The first of these expected crossings is the neutron AB $(i_{13/2})^2$ at $\hbar\omega\approx 0.28$ MeV followed by the first paired proton crossing $(h_{11/2})^2$ at $\hbar\omega \approx 0.43$ MeV. To identify the occupied orbitals at the nuclear Fermi surface experimentally, the band crossing frequency ω_c and the gain in aligned angular momentum Δi_x (or alignment), are used. The values of ω_c and Δi_x are generally extracted from alignment plots. The alignment of a rotational band is determined by subtracting a reference term (accounting for the behavior of the core) from the level spins, as discussed in Ref. [29]. In Fig. 4 the alignments of the yrast bands in the $N=90$ isotones ^{156}Dy, ^{157}Ho, and ^{158}Er are plotted. From this figure it is clear that the expected $i_{13/2}$ neutron alignment occurs in all three nuclei. The $h_{11/2}$ proton A_pB_p alignment is observed in ^{156}Dy and ^{158}Er but it is blocked in ^{157}Ho by the odd proton in an $h_{11/2}$ orbital. However, the B_PC_P proton crossing is seen in band $1a$ of ^{157}Ho and the start of the A_PD_P crossing is observed in band $1b$. The differences in the rate of increase of the alignment in these nuclei (e.g., ^{156}Dy, ^{158}Er) is due to the density of states at the proton Fermi surface.

As can be seen from Fig. 4, the alignment plots for ^{152}Dy(A) and ^{153}Dy differ from those of the $N=90$ isotones. Although the ^{152,153}Dy bands are observed to higher spins, there is no evidence for paired band crossings, such as the $\pi h_{11/2}$, at the higher rotational frequencies,. This suggests that the deformations of ^{152}Dy(A) and the ^{153}Dy band are somewhat different than that of ^{156}Dy.

A. Triaxial shapes in ^{152}Dy and ^{153}Dy

The nuclei ^{152}Dy and ^{153}Dy have similar level schemes, with the predominant de-excitation path from high spin

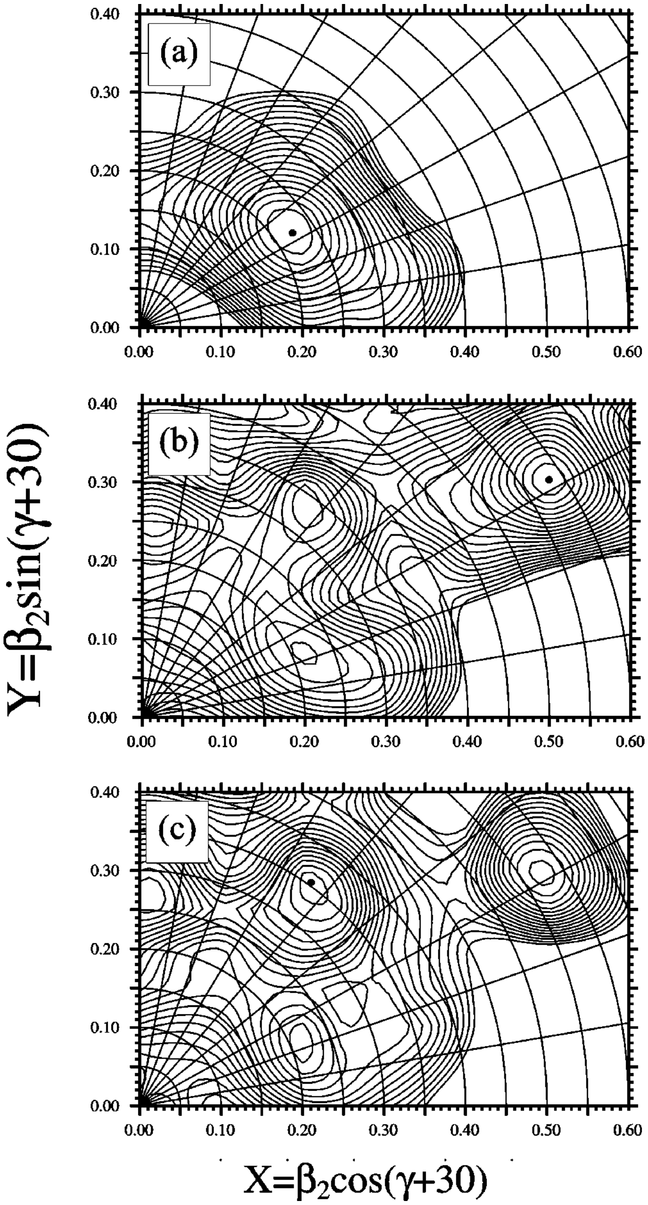

FIG. 3. TRS calculations for (a) the νAB configuration of ^{156}Dy at $\hbar\omega \approx 0.38$ MeV, (b) the νAB configuration of ^{152}Dy. Four distinct minima are identifiable, the superdeformed (at $\beta_2 \approx 0.59$, $\gamma \approx 1°$), two triaxial minima (at $\beta_2 \approx 0.31$, $\gamma \approx 19°$ and $\beta_2 \approx 0.25$, $\gamma \approx -15°$), and the single particle (at $\beta_2 \approx 0.11$, $\gamma \approx 50°$). (c) The $\nu AB\pi AF$ configuration in ^{152}Dy, showing the triaxial minimum at $\beta_2 = 0.36$ and $\gamma = 24°$.

through spherical single-particle states. Alternative paths exist via the collective bands that are observed to low spin, such as band *A* in ^{152}Dy [11] and the band in ^{153}Dy extended in this paper. The lowest states in these bands have been known for many years, with their extension to high spin made possible by developments in spectrometer technology. The ^{153}Dy band discussed here was observed in 1977 by Klein *et al*. [13], who compared it with similar bands in the $N=87$ isotones ^{149}Sm and ^{151}Gd. They carried out particle-rotor calculations [13] to determine the most probable structure and deformation parameters for the bands based on the

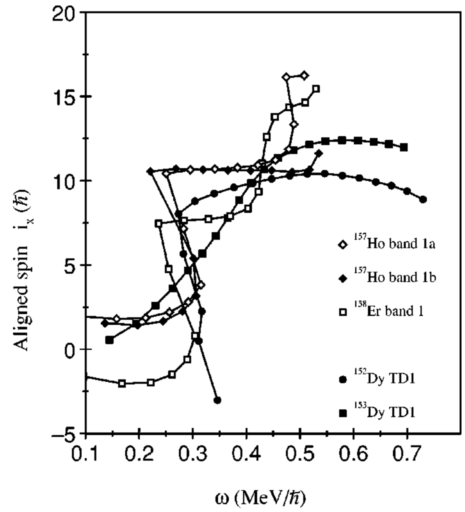

FIG. 4. The experimental aligned angular momentum as a function of rotational frequency for the yrast bands in the $N=90$ isotones ^{157}Ho and ^{158}Er. Also shown for comparison are the yrast TD bands in ^{152,153}Dy. The Harris parameters $\Im_0 = 32.1$ MeV$^{-1}\hbar^2$ and $\Im_1 = 34.0$ MeV$^{-3}\hbar^4$ were subtracted as a reference band.

$J^\pi = \frac{13}{2}^+$ band heads observed in their experiments. As a result of these calculations it was suggested that the bands were based on the occupation of three neutrons within the $i_{13/2}$ shell (see Sec. 4.1 of Ref. [13] for more details). In addition their calculations suggest that this band lies in a minimum in the nuclear PES defined by the deformation parameters $\beta_2 = 0.21$, $\beta_4 = 0.1$, and $\gamma = 23°$. These deformation parameters suggest that ^{153}Dy is more susceptible to the γ degree of freedom than ^{156}Dy. A similar scenario was predicted for ^{152}Dy [30], and noted in the paper reporting the extension of ^{152}Dy(*A*) to high spin by Nyako *et al.* [11]. Following the observation of superdeformed ($\beta_2 \approx 0.6$) states in ^{152}Dy [33] more detailed calculations were performed by Dudek *et al.* [31]. They predicted that ^{152}Dy(*A*) has deformation parameters of $\beta_2 = 0.25$ and $\gamma = 25°$, i.e., the band is triaxial.

We have carried out TRS calculations for ^{152}Dy [Fig. 3(b)] which show the presence of four distinct minima at high spin. Two of these minima can be readily identified, the first as superdeformed, the second belonging to single-particle states ($\gamma \approx 55°$). The other two minima are triaxial, one with a large positive γ and one with a smaller negative γ. Calculations performed with the cranked Woods-Saxon model indicate that the proton $h_{11/2}$ paired crossing, at moderate deformations ($\beta_2 \approx 0.25$), is expected to become quenched for large positive γ values, in agreement with the predictions of Dudek *et al.* [31]. In contrast, a paired proton crossing is expected if the γ degree of freedom is negative, making the bands more like those in ^{156}Dy [2] and ^{158}Er [32]. The assumption of a minimum with a negative γ degree of freedom was assumed in more recent work [12] and led to incorrect configuration assignments being attributed to the ^{152}Dy low deformation bands.

As discussed above, one method of comparing experimental and theoretical data is via alignment plots. An alignment gain of $\approx 15\hbar$ is observed at $\hbar\omega \approx 0.3$ MeV in ^{152}Dy band A (Fig. 4) with the major contribution to the alignment caused by $i_{13/2}$ neutrons (the AB crossing). If the remainder is due to the alignment of $h_{11/2}$ protons, as suggested in Refs. [11,12], then the total alignment at high frequency should be greater than that observed in the bands in ^{156}Dy [2] and ^{158}Er [32]. It is clear from Fig. 4 that the total alignment of ^{158}Er, after the proton alignment, is much greater than that for ^{152}Dy(A), which should not be the case if the paired proton crossing takes place in ^{152}Dy(A). It is much more likely that this additional alignment ($\approx 5\hbar$) in ^{152}Dy(A) at low frequency is due to the vibrational nature of ^{152}Dy at low spin. Hence it can be concluded that no alignment gain, due to a paired proton crossing, is observed in ^{152}Dy(A).

The band reported in ^{153}Dy exhibits similar properties to that of ^{152}Dy(A), suggesting similar deformation parameters, but with an extra alignment of $\approx 2.5\hbar$ at the highest frequencies. This can be reconciled with the extra $i_{13/2}$ neutron orbital that is occupied in ^{153}Dy. The crossing that is observed in ^{153}Dy at $\hbar\omega \approx 0.37$ MeV (Fig. 4) is consistent with the neutron BC paired crossing [5] as the AB neutron crossing is blocked by the odd $i_{13/2}$ neutron. With no other obvious alignments occurring, it can be concluded, as for ^{152}Dy(A), that no paired proton crossing is observed in this nucleus.

In order to determine the deformation of nuclear states their transition quadrupole moments (Q_t) have to be measured via lifetime experiments. No lifetime data are available on the reported band in ^{153}Dy, however, the Q_t for some of the states in ^{152}Dy(A) has been measured [12]. The deformation of these states can then be determined by relating the measured Q_t to the expected values of β and γ. However, a moderately deformed nucleus with $\beta_2 \approx 0.30$ and $\gamma \approx 20°$ exhibits a Q_t similar to a nucleus with a lower β_2 of 0.20 and γ close to zero. Thus, in this case, the Q_t data cannot distinguish between these two predicted deformations. Hence as no paired proton crossing is observed and the theoretical calculations predict triaxial shapes with positive γ it is concluded that both ^{152}Dy(A) and the band in ^{153}Dy are associated with the deformation parameters $\beta_2 \approx 0.30$ and $\gamma \approx 20°$.

The low deformation bands in ^{152}Dy were designated [11,12] as A, B, and C whereas the superdeformed bands have been labeled SD1, SD2, etc. This latter method provides a better rapid recognition of the deformation of the bands. Thus we have relabeled the triaxially deformed A, B, and C bands in ^{152}Dy as TD1, TD2, and TD3, and the ^{153}Dy band as TD1. This nomenclature is also consistent with the TSD designation for the triaxial superdeformed bands in ^{163,164,165}Lu [34,35].

B. Comparison with the triaxial SD bands in ^{163}Lu

A number of triaxial superdeformed bands have been observed in the nuclei ^{163,164,165}Lu [34,35], and the transition quadrupole moments of the strongest of these bands was determined to be $\approx 11e$b, consistent with a deformation of $\beta_2 \approx 0.4$ and $\gamma \approx 20°$. Theoretical studies of the nuclear PES of these lutetium nuclei with the Ultimate Cranker TRS code shows that these bands are associated with a triaxial shape ($\beta \approx 0.4$ and and $\gamma \approx 20°$) which led them to be described as superdeformed triaxial bands. One feature of these bands is that the magnitude of the dynamical moment of inertia ($\mathcal{J}^{(2)}$) is approximately constant at a value of $\approx 75\ \hbar^2$/MeV. This is higher than the values of $\approx 62\ \hbar^2$/MeV and $\approx 68\ \hbar^2$/MeV for the TD1 bands in ^{152,153}Dy over the range of $\hbar\omega$ from 0.5 to 0.6 MeV, Fig. 5.

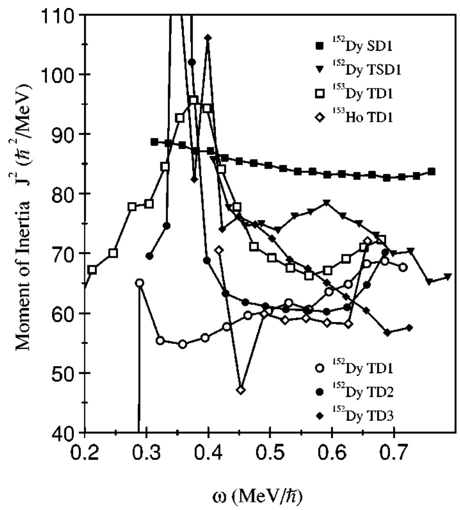

FIG. 5. The dynamical moment of inertia, $\mathcal{J}^{(2)}$ of the triaxial deformed bands in ^{152,153}Dy and ^{153}Ho. Also shown for reference is the $\mathcal{J}^{(2)}$ of the yrast SD band in ^{152}Dy.

In Refs. [34,35] it was pointed out that a key feature of the triaxial minimum in ^{163,164,165}Lu was the formation of a large neutron shell gap at $N=94$ and a large proton shell gap at $Z=71$. Also it was noted that the single-particle levels which increase greatly in energy as γ increases from 0° to 20° are the $\nu[402]\frac{3}{2}$ and the $\pi[402]\frac{5}{2}$ originating from the $2d_{3/2}$ orbital. At $\beta_2 \approx 0.4$ the $\nu[402]\frac{3}{2}$ crosses the Fermi surface when $N=94$ and thus is emptied, the $\pi[402]\frac{5}{2}$ has the same behavior at $Z=71$. Therefore transferring particles out of these particular orbitals when they are close to the Fermi surface produces a strong γ-driving effect.

In the case of ^{152,153}Dy, the $\nu[402]\frac{3}{2}$ orbital is again close to the Fermi surface when $N=86,87$ and $\beta_2 \approx 0.3$. It is this orbital which is emptied as γ increases from 0° to 20° [Fig. 7(a)]. Thus the major γ-driving effect has the same origin in both the ^{163,164,165}Lu and ^{152,153}Dy nuclei. The lower quadrupole deformation of ^{152,153}Dy, relative to the lutetium bands, is due primarily to having only $h_{11/2}$ proton orbitals occupied, whereas a strongly quadrupole driving $i_{13/2}$ proton orbital is also occupied in the lutetium nuclei when Z has increased to 71. Thus the minimum in the PES changes from $\beta_2=0.3$ to $\beta_2=0.4$. The dysprosium nuclei could be classified as moderately deformed triaxial and the lutetium nuclei as superdeformed triaxial, although it may have been better if this description had been reserved for the very large deformations with β_2 greater than 0.5.

C. ^{153}Ho band TD1

In the more axially deformed SD nuclei in the $A \approx 150$ region the $\mathcal{J}^{(2)}$ moments of inertia are smoothly varying and

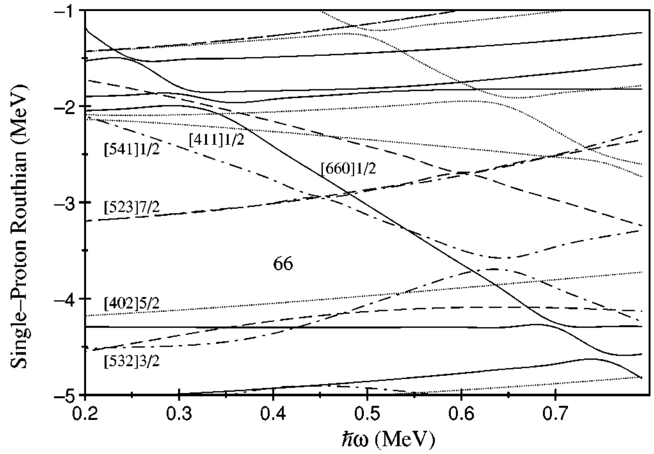

FIG. 6. Single-particle Routhians calculated for protons close to the Fermi surface in ^{152}Dy using a universal Woods-Saxon potential and the deformation parameters $\beta_2 = 0.30$, $\beta_4 = -0.004$, $\gamma = 18.0°$. Solid lines represent orbitals with $(\pi,\alpha) = (+,+/2)$; dotted lines those with $(\pi,\alpha) = (+,-1/2)$; dot-dash lines those with $(\pi,\alpha) = (-,+1/2)$; dashed lines those with $(\pi,\alpha) = (-,-1/2)$.

their magnitude and variation with frequency are characteristic of the different high-N orbital configurations. Thus these plots have been successfully used to assign high-N configurations to excited bands in neighboring nuclei [36]. The $\mathcal{J}^{(2)}$ of the TD1 triaxial bands in ^{152,153}Dy also vary smoothly (Fig. 5), and they have different features and magnitudes which are characteristic of the occupation of two and three $i_{13/2}$ neutron orbitals, respectively. Therefore the $\mathcal{J}^{(2)}$ plots of these bands in ^{152}Dy and ^{153}Dy are taken as references for the number of occupied $i_{13/2}$ neutron orbitals.

The $\mathcal{J}^{(2)}$ of the band in ^{153}Ho is shown in Fig. 5. The band is relatively short but over the observed region of frequency it is very similar in magnitude to TD1 (and TD2) of ^{152}Dy. Therefore it is concluded that only two $i_{13/2}$ neutron orbitals are occupied and also that the 67th proton does not drive the nuclear shape to either greater or smaller deformation. The single-particle proton Routhians are shown in Fig. 6 for a deformation of $\beta_2 = 0.3$ and $\gamma = 18°$. In the more neutron rich isotopes of holmium (e.g., ^{157}Ho) which have a deformation of $\beta_2 = 0.2$ and $\gamma = 0°$, the lowest energy band has the odd proton in the $[523]\frac{7}{2}$ orbital and excited bands with protons in the $[404]\frac{7}{2}$ and $[411]\frac{1}{2}$ orbitals. However, at a larger β_2 with γ, the down-sloping $2f_{7/2}\,[541]\frac{1}{2}$ orbital is lowest in the feeding region of the ^{153}Ho band ($\hbar\omega = 0.5$–0.6 MeV). This orbit crosses the $\pi[523]\frac{7}{2}$ at $\hbar\omega \approx 0.45$ MeV which could cause the discontinuity of $\mathcal{J}^{(2)}$ at this point (Fig. 5), and may be the cause of the associated decay out of the band. Although the occupation of the down-sloping $\pi[541]\frac{1}{2}$ orbital may increase the deformation slightly, it would not be as great as the adjacent $i_{13/2}\,[660]\frac{1}{2}$ orbital which drives the lutetium triaxial bands to $\beta_2 = 0.4$ with $\mathcal{J}^{(2)} \approx 75\hbar^2$/MeV. As $\mathcal{J}^{(2)}$ for the ^{153}Ho band is much lower in magnitude it is concluded that the $\pi[660]\frac{1}{2}$ orbital is not involved and neither is the $\pi[523]\frac{7}{2}$ as no evidence was found for a signature partner for the ^{153}Ho band despite a detailed search.

Thus it is proposed that the band in ^{153}Ho is triaxial with the odd proton in the $[541]\frac{1}{2}$ orbital. The band will have $\alpha = +\frac{1}{2}$ and the alignment is expected to be about 2–$3\hbar$ greater than the ^{152}Dy TD1 band. These conditions are satisfied by a spin assignment of $\frac{57}{2}^- \rightarrow \frac{53}{2}^-\hbar$ to the 806-keV transition in the ^{153}Ho band which gives an alignment gain of $\approx 2\hbar$ relative to the ^{152}Dy TD1 band (Fig. 8).

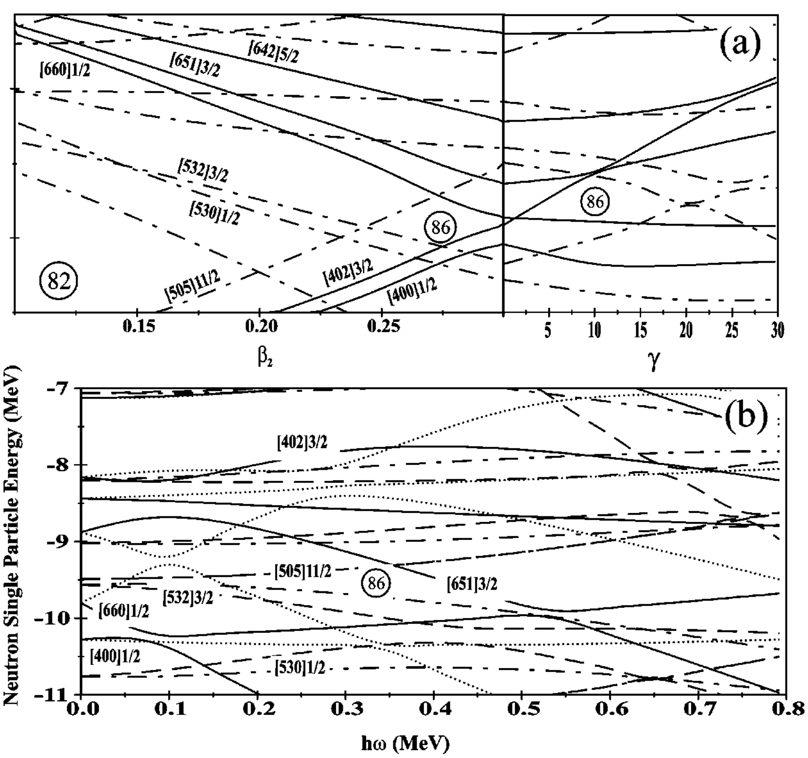

FIG. 7. Single-particle Routhians calculated for neutrons close to the Fermi surface in ^{152}Dy. (a) Shows the evolution of the neutron orbitals as a function of quadrupole deformation (β_2 and triaxiality, γ). (b) Shows the effect of rotation (ω) at a deformation of $\beta_2 = 0.30$ and $\gamma = 30°$. Solid lines represent orbitals with $(\pi,\alpha) = (+,+1/2)$; dotted lines those with $(\pi,\alpha) = (+,-1/2)$; dot-dash lines those with $(\pi,\alpha) = (-,+1/2)$; dashed lines those with $(\pi,\alpha) = (-,-1/2)$.

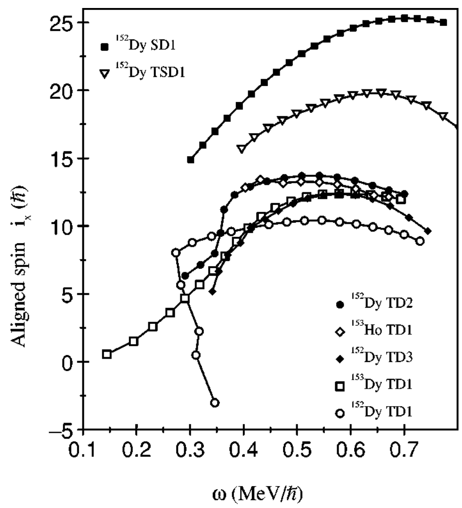

FIG. 8. The experimental aligned angular momentum as a function of rotational frequency for the TD and TSD bands in ^{152,153}Dy and ^{153}Ho. Also shown is the alignment for the yrast SD band in ^{152}Dy. The Harris parameters $\Im_0=32.1$ MeV$^{-1}\hbar^2$ and $\Im_1=34.0$ MeV$^{-3}\hbar^4$ were subtracted as a reference band.

D. ^{152}Dy band TD2

The excited bands in ^{152}Dy have different behaviors of their $\mathcal{J}^{(2)}$ moments of inertia, Fig. 5. Band TD2 has a constant $\mathcal{J}^{(2)}$ between $\hbar\omega=0.45$ and 0.62 MeV of $60\hbar^2$/MeV, a value very similar to the TD1 bands in ^{152}Dy and ^{153}Ho. This indicates that the band has only two $i_{13/2}$ neutron orbitals occupied. As the obvious neutron excitation is to the third $i_{13/2}$ orbital, it is concluded that the TD2 band is associated with a proton excitation. The most likely orbital to be occupied is the $\pi[541]\frac{1}{2}$, the same orbital involved in the ^{153}Ho band (see the previous section).

The proton hole must be in either the $[532]\frac{3}{2}$ $(\alpha=+\frac{1}{2})$ or the $[402]\frac{5}{2}$ $(\alpha=-\frac{1}{2})$ orbital. In the former case the band would have positive parity with $\alpha=0$, an alignment $\approx 2\hbar$ greater than the ^{153}Ho band, and it would interact with ^{152}Dy TD1 band when the $\pi[541]\frac{1}{2}$ $(\alpha=+\frac{1}{2}$ and $\pi[532]\frac{3}{2}$ levels cross at a frequency of $\hbar\omega=0.63$ MeV, Fig. 6. However, this crossing must occur at a higher frequency than that predicted, otherwise the ^{152}Dy TD1 band would show a strong increase in $\mathcal{J}^{(2)}$ at $\hbar\omega=0.63$ MeV. Also as band TD2 approaches this crossing the $\mathcal{J}^{(2)}$ moment of inertia would decrease if the hole was in the $\pi[532]\frac{3}{2}$ orbital whereas experimentally $\mathcal{J}^{(2)}$ shows a small sharp increase. Thus it is concluded that band TD2 is not associated with a $\pi[532]\frac{3}{2}$ hole. The proton hole must therefore be in the $[402]\frac{5}{2}$ orbital, giving the band negative parity and $\alpha=+1$, with an alignment slightly greater than the band in ^{153}Ho.

There is no obvious explanation for the small, sharp increase in $\mathcal{J}^{(2)}$ at high frequency as a proton effect. If it were associated with neutrons it could be due to the interaction of the $\nu[400]\frac{1}{2}$ orbital with the third $i_{13/2}$ $[651]\frac{3}{2}$ orbital. The reason this upturn in $\mathcal{J}^{(2)}$ is not seen in ^{152}Dy TD1 is probably associated with a slightly higher quadrupole deformation in band TD2 (due to the occupation of the down-sloping $[541]\frac{1}{2}$ orbital) causing the crossing to move to a lower frequency. The bump in $\mathcal{J}^{(2)}$ at $\hbar\omega=0.36$ MeV could be due to the interaction between the $[541]\frac{1}{2}$ and the $[523]\frac{7}{2}$ proton orbitals. The associated experimental alignment change of 3.5–4$\hbar$, Fig. 8, is consistent with the 2.5$\hbar$ alignment for the $[541]\frac{1}{2}$ orbital (determined from the ^{153}Ho band) and the negative alignment of $\approx 1\hbar$ associated with the vacated $[532]\frac{7}{2}$ orbital. This leads to a probable alignment of $\approx 3.5\hbar$ relative to the ^{152}Dy TD1 band which is satisfied if the 581-keV γ ray in TD2 is a $17^-\rightarrow 15^-$ transition.

This configuration and the associated spin assignment differs with that suggested in Ref. [12], which erroneously assumed that only one $i_{13/2}$ neutron orbital was occupied. As the spin assignments suggested here are $6\hbar$ greater than that suggested in Ref. [12], this means that the band has been incorrectly linked into the level scheme. We propose that the previously proposed strong linking transition of 581 keV is instead a member of the band, positioned as the final transition before de-excitation. The de-excitation of this band to the single-particle states is most probably distributed over several different decay paths.

E. ^{152}Dy band TD3

The $\mathcal{J}^{(2)}$ moment of inertia of ^{152}Dy band TD3 has a very different shape and magnitude compared to ^{152}Dy TD1 band, Fig. 5. However, it has similarities with band TD1 in ^{153}Dy which has three $i_{13/2}$ neutron orbitals occupied. The zigzag discontinuity at $\hbar\omega=0.38$ MeV in TD3 is associated with a small shift of 4.5 keV in the energy of the state which follows the 788-keV γ ray. It is known experimentally that, at this point, part of the intensity of the band de-excites into the single-particle states as the band is observed in coincidence with γ rays below the 17^+ isomer. Thus as the $\mathcal{J}^{(2)}$ moment of inertia is very similar to that of the ^{153}Dy band between frequencies of 0.4 and 0.6 MeV it is concluded that TD3 has three $i_{13/2}$ neutron orbitals occupied. Compared with the ^{152}Dy TD1 band the hole is in either one of the signature partners of the $[532]\frac{3}{2}$ orbital or the $[400]\frac{1}{2}$ $(\alpha=+\frac{1}{2})$ orbital. A complication in the former possibility is that the frequency of the interaction between the $\alpha=-\frac{1}{2}$ signature components of the $[532]\frac{3}{2}$ and $[530]\frac{1}{2}$ orbitals varies rapidly with small changes of deformation. If the hole is in the $[532]\frac{3}{2}$ $(\alpha=-\frac{1}{2})$ orbital then it is expected that the $\mathcal{J}^{(2)}$ of TD3 would follow closely that of the ^{153}Dy band at all frequencies. However, it deviates strongly at high frequencies. If the hole is in the $\nu[532]\frac{3}{2}$ $(\alpha=-\frac{1}{2})$ orbital then the $\mathcal{J}^{(2)}$ of TD3 would closely match that of the ^{153}Dy band except possibly at lower frequencies where the interaction with the $\nu[530]\frac{1}{2}$ could occur thus leading to an increase in $\mathcal{J}^{(2)}$. However, again there is no explanation for the decrease in $\mathcal{J}^{(2)}$ at the high frequencies.

At a deformation of $\beta_2\approx 0.30$ and $\gamma\approx 20°$ the crossing between the strongly up-sloping $\nu[400]\frac{1}{2}$ and the strongly down-sloping $\nu[651]\frac{3}{2}$ orbitals occurs at a frequency of $\hbar\omega = 0.6$ MeV, although the exact position of the crossing changes rapidly with small changes in β_2, Fig. 7. Indeed, as no large increase in $\mathcal{J}^{(2)}$ is observed in ^{152}Dy band TD1 up to $\hbar\omega = 0.7$ MeV, it is concluded that this crossing must occur at a frequency greater than 0.7 MeV. If the hole is in the $\nu[400]\frac{1}{2}$ $(\alpha = +\frac{1}{2})$ orbital, then the $\mathcal{J}^{(2)}$ should match that of the ^{153}Dy band, except possibly at the highest frequencies where the first indication of the crossing between the $\nu[400]\frac{1}{2}$ and the $\nu[651]\frac{3}{2}$ could occur. This would result in a small reduction of $\mathcal{J}^{(2)}$ compared to the ^{153}Dy band and this feature is observed experimentally. The crossing band is the ^{152}Dy TD1 which has the $\nu[400]\frac{1}{2}$ orbital occupied and thus the slow increase in $\mathcal{J}^{(2)}$ of TD1 at the high frequencies could also be due to the first indication that this crossing is being approached.

In conclusion, it is considered that the data are best explained by the ^{152}Dy TD3 having the configuration involving the excitation of a neutron from the $[400]\frac{1}{2}$ orbital to the $[651]\frac{3}{2}$ orbital. The alignment of TD3 is very similar to the ^{153}Dy band, and thus it is suggested that the 683-keV γ ray is a $18^+ \rightarrow 16^+$ transition, which produces the alignments shown in Fig. 8.

This explanation differs from that suggested previously, in that three $\nu i_{13/2}$ orbitals are occupied, as opposed to the one suggested in Ref. [12]. As the spin assignments proposed in this paper are $4\hbar$ higher than that suggested previously [12] this means that the band has been incorrectly linked into the level scheme of ^{152}Dy. The previously proposed 690- and 526-keV linking transitions must link into the decay scheme in a different way.

F. ^{152}Dy band TSD1

Dagnal *et al.* [36] reported the observation of six collective bands which decayed through the 17^+ isomer in ^{152}Dy. Five of these bands had $\mathcal{J}^{(2)}$ moments of inertia with a magnitude greater than 80 $\hbar^2$/MeV at high frequencies and thus were clearly associated with superdeformed states ($\beta_2 \approx 0.6$). The other band (labeled SD3) had $\mathcal{J}^{(2)}$ below 80 $\hbar^2$/MeV and they could not definitely assign the band to an excitation producing a characteristic $\mathcal{J}^{(2)}$ of a superdeformed high-N configuration in a neighboring nucleus. The $\mathcal{J}^{(2)}$ of this band (Fig. 5) is also much larger than the proposed triaxial bands in ^{152,153}Dy. However, as it lies between 75 and 78 $\hbar^2$/MeV in the frequency range $\hbar\omega = 0.45$–0.65 MeV, it has a similar magnitude to the moments of inertia of the superdeformed triaxial bands in ^{163,164,165}Lu [34,35]. Recently a new SD band with a $\mathcal{J}^{(2)}$ of over 80 $\hbar^2$/MeV has been reported by Lagergren *et al.* [37] in ^{154}Er, and they propose that the original SD band, which has a lower $\mathcal{J}^{(2)}$ of ≈ 76 $\hbar^2$/MeV, is a superdeformed triaxial band similar to those in the lutetium isotopes. The $\mathcal{J}^{(2)}$ of this TSD band in ^{154}Er is constant between $\hbar\omega = 0.45$ and 0.6 MeV, it has a discontinuity at $\hbar\omega = 0.65$, and a steady increase of $\mathcal{J}^{(2)}$ below $\hbar\omega = 0.45$ MeV. Thus SD3 in ^{152}Dy exhibits the magnitude of $\mathcal{J}^{(2)}$ which is characteristic of the superdeformed triaxial bands in ^{154}Er and ^{163,164,165}Lu and it is proposed that it is also a superdeformed triaxial band. Accordingly it has been relabeled as TSD1 in ^{152}Dy.

The slow decrease of $\mathcal{J}^{(2)}$ above $\hbar\omega = 0.65$ in TSD1 is a unique observation. It probably does not have the same origin as the decrease of $\mathcal{J}^{(2)}$ in band TD3, which has been linked to the crossing of the $[651]\frac{3}{2}$ and $[400]\frac{1}{2}$ neutron orbitals, as at the higher deformation of $\beta_2 = 0.36$ this crossing has moved to a much lower frequency and, indeed, could be responsible for the increase in $\mathcal{J}^{(2)}$ at $\hbar\omega = 0.4$ MeV in both TSD1 and the band in ^{154}Er. A more likely explanation for the decrease in $\mathcal{J}^{(2)}$ at high frequency is the approach of the crossing of the filled $[660]\frac{1}{2}$ $(\alpha = +\frac{1}{2})$ with the empty $[402]\frac{5}{2}$ proton orbitals. This band TSD1 is most probably based on an $i_{13/2}$ proton excitation excitation from band TD3 (which has $3i_{13/2}$ neutrons) giving an additional proton alignment of ≈ 4–$5\hbar$, plus the $[541]\frac{1}{2}$ proton excitation observed in band TD2 which provides an additional alignment gain of $\approx 2.5\hbar$. The resulting total alignment gain of $\approx 7\hbar$ relative to band TD3 indicates a spin assignment of 31^-–29^- for the 793-keV transition which yields the alignment plot shown in Fig. 8. Relative to ^{152}Dy band TD1 the proton configuration is probably $[402]\frac{5}{2}^{-2}$ $[541]\frac{1}{2}[660]\frac{1}{2}$ and the neutron configuration $[400]\frac{1}{2}^{-1}[651]\frac{3}{2}$ producing a band with negative parity and $\alpha = +1$. One difference in the features of TSD1 in ^{152}Dy is that it is observed up to $\hbar\omega = 0.8$ MeV compared with $\hbar\omega = 0.65$ MeV in ^{154}Er and under 0.6 MeV in ^{163,164,165}Lu [34,35]. TRS calculations for this configuration [Fig. 3(c)] indicate a minimum in the PES at a deformation of $\beta_2 \approx 0.36$ and $\gamma \approx 20°$ that is only present at high spin, in agreement with the experimental data.

This interpretation provides an explanation for this band that was lacking in Ref. [36], and modifies the band head spins, lowering them by $7\hbar$.

V. CONCLUSIONS

In conclusion, a new rotational band has been observed in ^{153}Ho that exhibits characteristics similar to bands observed in ^{152}Dy. In addition, the $i_{13/2}$ band in ^{153}Dy has been extended to higher spins. These bands are discussed in terms of the cranked shell model, and resulted in a reinterpretation of the configurations previously proposed for the bands in ^{152}Dy. On the basis of the theoretical calculations coupled to the absence experimentally of an $h_{11/2}$ proton crossing, these bands have been assigned as triaxially deformed and in the case of one band in ^{152}Dy as triaxially superdeformed. The similarity with the triaxial superdeformed bands in the lutetium isotopes and in ^{154}Er is discussed. Proposals have been made for the configuration of the bands relative to the TD1 band in ^{152}Dy, this has led to tentative spin assignments. In order to confirm these assignments for the excited bands in ^{152}Dy and ^{153}Ho, a large data set is required to observe the linking transitions between these bands and the single-particle states.

ACKNOWLEDGMENTS

We wish to thank the crew of the Vivitron for providing the high quality beams. Two of us (D.E.A. and M.B.S.) acknowledge the support of the EPSRC (U.K.). EUROGAM is jointly funded by EPSRC (U.K.) and IN2P3 (France). D.M.C. acknowledges support from the EPSRC. This work was supported in part by the Canadian Natural Sciences and Engineering Council.

[1] W.C. Ma *et al.*, Phys. Rev. Lett. **61**, 46 (1988).
[2] M.A. Riley *et al.*, Nucl. Phys. **A486**, 456 (1988).
[3] B.K. Agrawal, T. Sil, S.K. Samaddar, and J.N. De, Phys. Rev. C **63**, 024002 (2001).
[4] D.E. Appelbe *et al.*, Phys. Rev. C **56**, 2490 (1997).
[5] D.C. Radford *et al.*, Nucl. Phys. **A545**, 665 (1992).
[6] M.A. Rizzutto *et al.*, Phys. Rev. C **55**, 1130 (1997).
[7] Suresh Kumar Patra and Prafulla Kumar Panda, Phys. Rev. C **47**, 1514 (1993).
[8] W.F. Mueller, H.J. Jensen, W. Reviol, L.L. Riedinger, C.-H. Yu, J.-Y. Zhang, W. Nazarewicz, and R. Wyss, Phys. Rev. C **50**, 1901 (1994).
[9] X.-L. Han and C.-L. Wu, At. Data Nucl. Data Tables **63**, 117 (1996).
[10] R. B. Firestone and V. S. Shirley, *Table of Isotopes*, 8th ed. (Wiley, New York, 1996), Vol. II.
[11] B.M. Nyako *et al.*, Phys. Rev. Lett. **56**, 2680 (1986).
[12] M.B. Smith *et al.*, Phys. Rev. C **61**, 034314 (2000).
[13] P. Kleinheinz, A.M. Stefanini, M.R. Maier, R.K. Sheline, R.M. Diamond, and F.S. Stephans, Nucl. Phys. **A283**, 189 (1977).
[14] D.C. Radford *et al.*, Phys. Lett. **126B**, 24 (1983).
[15] J. K. Johansson *et al.*, Proceedings of the International Conference on ''Nuclear Structure of the Nineties,'' Oak Ridge, TN, 1990, Vol. 1 p. 132.
[16] C.W. Beausang and J. Simpson, J. Phys. G **22**, 527 (1996).
[17] C.W. Beausang *et al.*, Nucl. Instrum. Methods Phys. Res. A **313**, 37 (1992).
[18] G. Duchêne *et al.*, Nucl. Instrum. Methods Phys. Res. A **432**, 90 (1999).
[19] D.C. Radford, Nucl. Instrum. Methods Phys. Res. A **361**, 297 (1995).
[20] J.K. Johansson *et al.*, Phys. Rev. Lett. **63**, 2200 (1989)
[21] D.S. Haslip, G. Hackman, and J.C. Waddington, Nucl. Instrum. Methods Phys. Res. A **345**, 534 (1994).
[22] J.N. Wilson and D.C. Radford, Nucl. Instrum. Methods Phys. Res. A **385**, 108 (1997).
[23] K.S. Krane, R.M. Steffan, and R.M. Wheeler, Nucl. Data Tables **11**, 351 (1973).
[24] M. Kortelahti *et al.*, Phys. Lett. **131B**, 305 (1983).
[25] P. Kleinheinz, R.K. Sheline, M.R. Maier, R.M. Diamond, and F.S. Stephens, Phys. Rev. Lett. **32**, 68 (1974).
[26] J.F.W. Jansen, M.J.A. De Voigt, Z. Sujkowski, and D. Chmielewska, Nucl. Phys. **A321**, 365 (1979).
[27] W. Nazarewicz, R. Wyss, and A. Johnson, Nucl. Phys. **A503**, 285 (1989).
[28] H. Emling *et al.*, Nucl. Phys. **A419**, 187 (1984).
[29] R. Bengtsson and S. Frauendorf, Nucl. Phys. **A314**, 27 (1979).
[30] J. Dudek and W. Nazarewicz, Phys. Rev. C **31**, 298 (1985).
[31] J. Dudek, B. Herskind, W. Nazarewicz, Z. Symanski, and T.R. Werner, Phys. Rev. C **38**, 940 (1988).
[32] M.A. Riley *et al.*, Phys. Lett. **135B**, 275 (1984).
[33] P.J. Twin *et al.*, Phys. Rev. Lett. **57**, 811 (1986).
[34] H. Schnack-Petersen, Nucl. Phys. **A594**, 175 (1995).
[35] S. Tormanen *et al.*, Phys. Lett. B **454**, 8 (1999).
[36] P.J. Dagnall *et al.*, Phys. Lett. B **335**, 313 (1994).
[37] K. Lagergren *et al.*, Phys. Rev. Lett. **87**, 022502 (2001).